RESEARCH PAPER

Effects of Cement and Nanoclay on the Characteristics of the Sand with Non-Plastic Fine Materials

Vahid Momeni Helali[1] · Reza Noorzad[1]

Abstract

Soil stabilization with cement is one of the most widely used methods in construction projects. Nowadays, the use of new and environmentally friendly materials, such as nanoparticles, has attracted the attention of geotechnical engineers. Hence, in the present study, cement and nanoclay (NC) were added to silty sand to improve the soil properties through various tests, including standard Proctor compaction, unconfined compressive strength (UCS), and unconsolidated-undrained (UU) triaxial tests. Evaluations were performed for different percentages of cement (4, 6, and 8% by dry weight of the mixed soil) and NC (0, 0.5, 1, and 2% by dry weight of the cement, as an additive and replacement materials). Curing time for UCS tests was 7, 14, and 28 days, and for UU triaxial test was 14 days. The results of the standard Proctor compaction tests showed that with increase in the cement percentage, the maximum dry unit weight increased, and the optimum moisture content (OMC) decreased. Results of the UCS tests indicated that by increasing the cement percentage, the UCS enhanced, and the samples exhibited brittle behavior. Moreover, the NC had no significant effect on the UCS as well as the brittle behavior of the cement-stabilized samples. The results of the UU triaxial tests showed that not only the cohesion (C) but also the internal friction angle (φ) improved with increase in the cement percentage, in which the increase in the C was more significant in comparison with the φ.

Keywords Soil stabilization · Cement · Nanoclay · Unconfined compressive strength · Shear strength parameters

1 Introduction

In many construction projects, there are soils with inappropriate characteristics for good performance. These soils can be improved by various methods to obtain the required performance and strength. Among various stabilizers, cement is widely used in soil stabilization except for organic soils. The best effect of cement is observed in sandy and gravelly soils, but in most sandy soils, there are also non-plastic fine grains. Therefore, the stabilization of these types of soils using cement is a suitable method (Sariosseiri and Muhunthan, 2009). Nowadays, in addition to traditional stabilizers, nanoscale stabilizers are also used to stabilize the soil. Soil nanoparticles are typically the smallest particles in the soil environment, with sizes between 1 and 100 nm. These materials have a very high surface area because of their very small size. Therefore, they react very actively with other soil particles. For this reason, when these particles are used in the soil environment, the physicochemical behavior and engineering properties of the soil will be significantly affected (Zhang, 2007). Schnaid et al. (2001) investigated the effect of cement on the stress–strain and strength behavior of silty sand using various tests. The results showed that the unconfined compressive strength (UCS) of the cemented samples can be directly used as a reference variable to express the cementation degree. Moreover, they expressed the shear strength of cemented samples as a function of two parameters, including the effective internal friction angle and UCS. Iranpour and Haddad (2016) added various nanoparticles, including nanoclay (NC), nanocopper, nanoalumina, and nanosilica to the clay of low plasticity (CL). They concluded that an increase in nanoparticles to more than 0.1% of the soil dry weight can have a negative effect on collapse potential. The lowest amount of the collapse potential was obtained using 0.1% NC. Also, nanocopper,

✉ Reza Noorzad
  rnoorzad@nit.ac.ir; rn0864@gmail.com

  Vahid Momeni Helali
  vmh0191@gmail.com

1 Faculty of Civil Engineering, Babol Noshirvani University of Technology, P.O. Box 484, Babol 4714871167, Iran

nanoalumina, and nanosilica were effective in decreasing the collapse potential. Kutanaei and Choobbasti (2017) found that the inclusion of Portland cement to sandy soil changes soil behavior to a more brittle one. With the increase in cement content, maximum dry density, the secant modulus of deformation (E_{50}), and UCS increased while optimum moisture content (OMC) decreased. They also observed that increasing the percentage of nanosilica up to 8% resulted in a noticeable increase in the ultrasonic pulse velocity. Moreover, the addition of fibers to the cemented sand decreased E_{50} and increased energy absorption capacity and UCS values. Zomorodian et al. (2017) found that with the addition of kerosene equal to eight and more weight percent of soil (wt. %) to sandy lean clay soil, strength, and stiffness decrease substantially. Addition of 1 wt. % NC or 1.5 wt. % nanosilica to this soil produced the best enhancement in strength. Compared with nanosilica, NC was considered to be more effective in increasing the uniaxial strength/stiffness due to its lower optimum value needed for both the clean and polluted soil. Tabarsa et al. (2018) reported that with adding NC to fine-grained soil, cohesion (C), plasticity index, and OMC increased while internal friction angle (φ) and maximum dry unit weight of soil decreased. Moreover, by performing field study, they expressed that the lowest amount of erosion was achieved by adding 2% NC to the soil. Baziar et al. (2018) observed that by adding 3% NC to the soil, the maximum dry unit weight increased, and hydraulic conductivity reduced. Moreover, the self-healing of the samples improved and the maximum shear strength increased 30% after 10 days of cracking while the unstabilized samples retrieved only 11% of their maximum shear strength at the same time. With the increase in the NC content to 4%, swelling and the plasticity index increased while no significant change was observed for the liquid limit. Shahidi et al. (2019) investigated the effects of NC and organoclay on the behavior of clayey sand polluted with gas oil. The results of the Atterberg limits tests indicated the return of plasticity characteristics and a decrease in hydrophobia of polluted soil using these additives. Also, the durability tests showed the appropriate effect of nanoparticles on the durability increase in the stabilized polluted specimens for various freeze–thaw cycles. Besides, the initial strength of the stabilized specimens increased their stability and durability versus temperature alterations. By conducting a series of experiments, Vranna and Tika (2020) found that with increase in the percentage of cement, the UCS and tensile strength increased. The tensile strength is at least 10 times lower than the UCS. They also observed that an increase in cementation leads to the improvement of the undrained shear strength and the reduction of the soil contraction. Furthermore, cementation may lead to the change of soil liquefaction from flow type into cyclic mobility one. The influence of cement percentage on the critical state of cemented sand may be considered analogous to the influence of the non-cementitious fines on the critical state lines of uncemented sand. The effect of fine content on the strength and stiffness of cement-stabilized sand was investigated by Moon et al. (2020). The results showed that by adding a low amount of kaolinite, the strength and stiffness of cement-stabilized soil was significantly increased. They stated that this issue is related to the improvement of density with kaolinite acting as a filler material, which leads to the increase in contact points between the particles.

2 Experimental Program

2.1 Materials

The sand used was derived from Babolsar city, in the north of Iran. The color of this type of sand is dark, and its particle size distribution curve is shown in Fig. 1. To make the sand more uniform and due to the existence of wastes in it, this sand was passed through sieve No. 40. The physical properties of Babolsar sand are presented in Table 1. The silt employed in this research is Firuzkuh silt, which was passed through sieve No. 200 before use. Figure 1 indicates the particle size distribution curve of this soil. The physical properties of Firuzkuh silt are shown in Table 1. The particle size distribution of the MS (containing 85% Babolsar sand and 15% Firuzkuh silt) is indicated in Fig. 1. The physical properties of the MS are also presented in Table 1. The cement used is Portland cement type II of Neka cement factory, Mazandaran, Iran. The cement was first passed through sieve No. 200. The physical and chemical properties of this cement are shown in Tables 2 and 3, respectively. The NC utilized in this study is the product of Sigma-Aldrich factory, Germany, with the commercial name of Nanoclay Montmorillonite, Na^+, K (10). The physical and chemical characteristics of this NC are indicated in Tables 4 and 5, respectively. Figure 2 shows the scanning electron microscope (SEM) image of NC. In this research, 18 standard Proctor compaction tests, 63 UCS tests, as well as 21 unconsolidated-undrained (UU) triaxial tests were performed on the mixed soil containing 85% sand and 15% silt (MS) with the addition of stabilizers including cement and NC.

2.2 Sample Preparation

In this study, sand and silt were first manually mixed in a dry state. Then, cement was added and blended until the mixture reached a uniform color. At the next step, NC was added and mixed for five minutes. Then, the required amount of water (OMC), obtained from the results of the standard Proctor compaction tests, was added to the soil–cement–NC mixture. In order to achieve a homogeneous mixture, the mixing process was manually performed for five minutes

Fig. 1 Particle size distribution curves for sand, silt, and MS
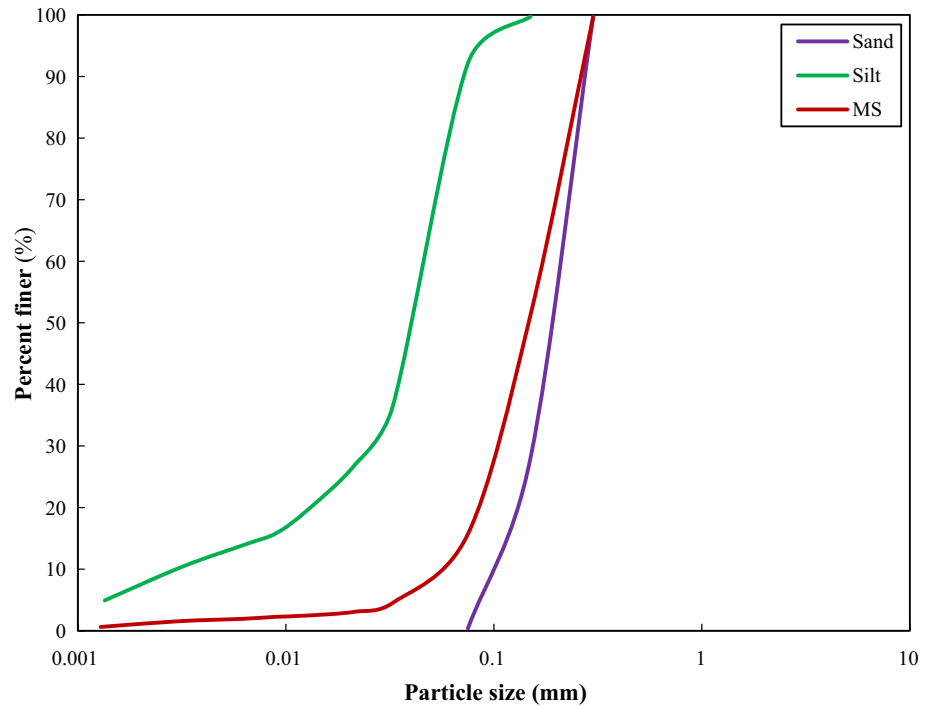
Table 1 Physical properties of soils

Characteristics	Standard designation	Sand	Silt	MS
Specific gravity (Gs)	ASTM D854 (2014)	2.74	2.70	2.73
Effective grain size, D10 (mm)	–	0.101	–	0.053
Medium grain size, D50 (mm)	–	0.196	0.043	0.147
Coefficient of uniformity (Cu)	–	2.14	–	2.81
Coefficient of curvature (Cc)	–	1.08	–	0.63
Passing No. 200 sieve (%)	ASTM D422 (2007)	0.36	92.14	15.67
Atterberg limits (%)	ASTM D4318 (2017)			
Liquid limit, LL		–	23	–
Plastic limit, PL		–	20	–
Plasticity index, PI		–	3	–
Unified soil classification system (USCS)	ASTM D2487 (2017)	SP	ML	SM

Table 2 Physical properties of cement

Property	Value
Blaine specific surface (m2/kg)	305
Initial setting time (min)	115
Final setting time (min)	195
Specific gravity	3.15
Expansion (autoclave) (%)	0.05
Compressive strength (kPa)	
3 days	18,142.3
7 days	28,929.6
28 days	38,932.4

and then continued using an electric mixer. Wet tamping method was used for sample preparation in this study. The obtained homogeneous mixture was divided into five equal portions, and each portion was kept in plastic wraps to prevent moisture loss. Then, each part was poured into a mold, with a diameter of 50 mm and a height of 100 mm, and compacted using a metal tamper. To create a better bonding between the layers, surface of each layer was scarified before pouring the next layer. After the compaction process, the sample was removed from the mold using a jack. In unconfined compressive strength tests, the compacted specimens were sealed in plastic wraps to avoid considerable variations

Table 3 Chemical and mineral compositions of cement

Property	Value (%)
SiO2	21.90
AL2O3	4.86
Fe2O3	3.30
MgO	1.15
CaO	63.32
SO3	2.10
Na2O	0.36
K2O	0.56
CaCO3	–
Loss on ignition (LOI)	2.40
Mineral composition	
C3S	47.98
C2S	26.61
C3A	7.30
C4AF	10.04

Table 4 Physical properties of NC

Property	Value/description
Mineral	Montmorillonite
Density (gr/cm3)	0.5–0.7
Particle size (nm)	1–2
Specific surface area [SSA (m2/gr)]	220–270
Electrical conductivity (MV)	− 25
Cation exchange capacity (Meg/100 gr)	48
Space between the particles (A°)	60
Color	Pale yellow
Moisture (%)	1–2

Table 5 Chemical compositions of NC

Chemical composition	Value (%)
SiO2	50.95
AL2O3	19.60
Fe2O3	5.62
MgO	3.29
CaO	1.97
Na2O	0.98
K2O	0.86
TiO2	0.62
Loss on ignition (LOI)	15.45

of moisture content and kept in a room with controlled temperature under different curing times (7, 14, and 28 days). All the samples were prepared with OMC and 95% of the maximum dry unit weight. Table 6 presents the number of tests in this study.
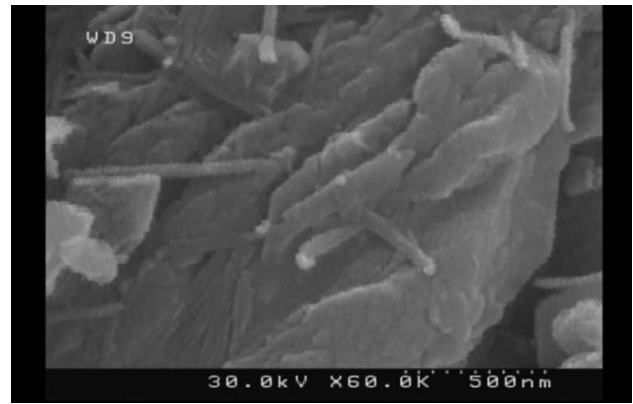
Fig. 2 SEM image of NC

2.3 Standard Proctor Compaction Tests

In this study, standard Proctor compaction tests for sand and MS according to ASTM D698-12 (2012) standard (Method A), and for MS with different percentages of cement)4, 6, and 8% by the dry weight of the MS) in two conditions including immediate and with 24 h delay according to ASTM D558-19 (2019) standard (Method A) were performed. Finally, the values of maximum dry unit weight and OMC for each combination were determined. It should be noted that standard Proctor compaction tests for each combination were carried out more than once, where the results will be presented in Sect. 3.1. The purpose of considering 24 h delay in this study is that due to the executive problems in many construction projects, there may be an interval between mixing and compaction. Therefore, the effects of this time interval on the standard Proctor compaction test parameters are studied.

2.4 Unconfined Compressive Strength Tests

The unconfined compressive strength tests on MS samples with the stated percentages of cement in the standard Proctor compaction tests and NC (0, 0.5, 1, and 2% by dry weight of the cement, as an additive and replacement materials) were carried out according to ASTM D2166-16 (2016) [18] standard at various curing times of 7, 14, and 28 days. The tests were performed by the strain-controlled method with the axial strain rate of 1.2% per minute. It should be explained that according to the strength of the samples (depending on the percentages of cement and NC, as well as the curing time), 5 and 10 kN load rings were used.

2.5 UU Triaxial Tests

In the UU triaxial test, the sample should be saturated because the calculation of the sample cross-sectional area

Table 6 Number of tests in this study

Test	Soil	Cement content (%)	Nanoclay content (%)	Curing time (days)	Confining pressure (kPa)	Number of tests	Total
Standard Proctor compaction test	Sand	–	–	–	–	1 + 2(repeated)	18
	SM	–		–		1 + 2(repeated)	
	SM	For immediate condition (4, 6, and 8%)		–		3 + 3(repeated)	
		With 24 h delay (4, 6, and 8%)		1		3 + 3(repeated)	
Unconfined compressive strength (UCS) test	SM	4, 6, and 8%	–	7, 14, and 28	–	9	63
			As an additive material (0, 0.5, 1, and 2%)			27	
			As a replacement material (0, 0.5, 1, and 2%)		–	27	
Unconsolidated-undrained (UU) triaxial test	SM	–	–	14	600, 700, and 800	3	21
	SM	Usual condition (4, 6, and 8%)				9	
	SM	Water-submerged condition (4, 6, and 8%)				9	

and the deviatoric stress are performed assuming that the sample volume does not change during the test. On the other hand, back pressure cannot be used to saturate the sample. Therefore, the only way to saturate the sample is to use high confining pressures (CPs). The high CPs cause the air bubbles to dissolve in the water as much as possible, resulting in the sample saturation and closure of the micro-cracks in the sample. Accordingly, to evaluate the short-term behavior of the MS with the mentioned percentages of cement at previous sections, UU triaxial tests were performed according to ASTM D2850-15 (2015) standard. The UU triaxial tests were conducted by the strain-controlled method with axial strain rate of 1% per minute. The samples were tested at the curing time of 14 days under the CPs of 600, 700, and 800 kPa. Based on the strength of the samples, for the unstabilized (MS) and stabilized samples, 10 and 28 kN load rings were used, respectively. It is necessary to explain that the samples were tested after curing time, which from now on referred to as usual stabilized (US) samples. Also, in this study, the samples were placed in a water container for 48 h before testing, after which the samples were extracted from the water and the surface of the samples was absorbed by an absorbent cloth and then was tested, which from now on these samples referred to as water-submerged stabilized (WSS) samples.

3 Results and Discussion

3.1 Standard Proctor Compaction Tests

It can be observed in Fig. 3 that with replacing 15% silt with sand, the maximum dry unit weight increases and the OMC decreases. The denser packing, which occurs through filling the void spaces with the addition of fines leads to the increase in the maximum dry unit weight and the reduction of OMC (less water is required to fill the voids between the sand particles). These results have good agreement with the ones reported by Deb et al. (2010).

It is also observed that with adding cement to MS, the maximum dry unit weight increases and the OMC decreases. The maximum dry unit weight increase can be attributed to two reasons. The first reason is that the specific gravity of cement (3.15) is higher than MS (2.73), which results in increasing the maximum dry unit weight. Similar results were found by previous researchers (Kutanaei and Choobbasti, 2017; Al-Homidy et al., 2016; Al-Aghbari et al., 2009; Hasanzadeh and Shooshpasha, 2019; Hasanzadeh and Shooshpasha, 2020). The second reason is the difference in the particle size of the MS and cement. Since the cement particles are much smaller than the MS particles, the cement particles fill the voids in the MS and produce a denser and more coherent structure, which have also been

Fig. 3 SPC curves for sand, MS and MS with different cement contents
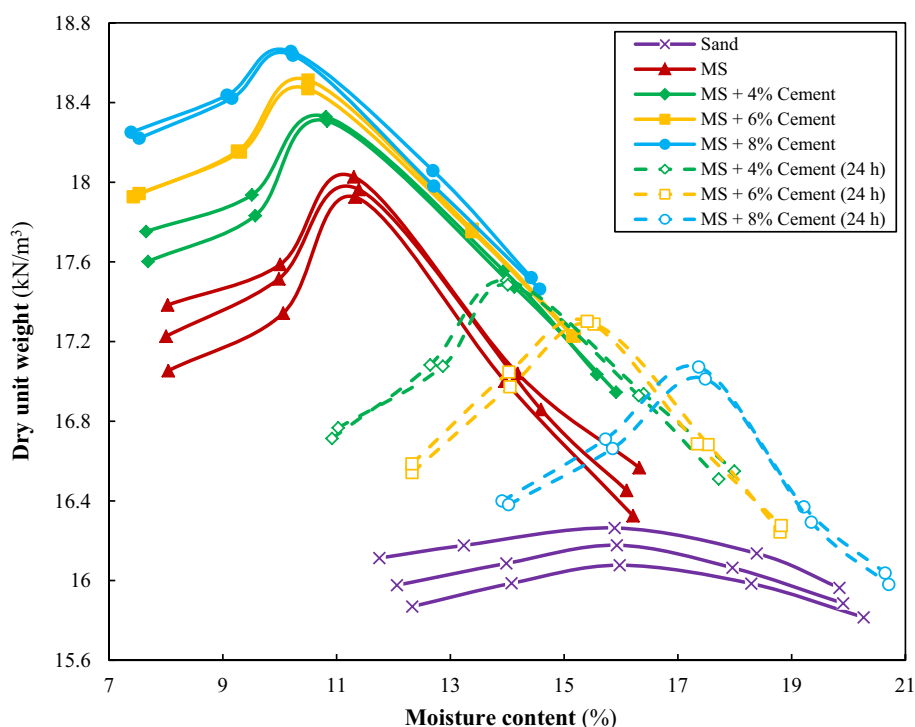
recognized by other researchers (Kutanaei and Choobbasti, 2017; Al-Aghbari et al., 2009; Hasanzadeh and Shooshpasha, 2019, 2020).

The decrease in OMC may be due to the self-desiccation of the water. When the water movement to the cement paste is prevented, the water is consumed in the hydration reaction until too little is remained for saturation of the solid surfaces. Hence, the relative humidity within the paste decreases, as also observed by other researchers (Hasanzadeh and Shooshpasha, 2019, 2020; Mengue et al., 2017a). Also, the decrease in OMC indicates that the cement acts as a lubricant as well as its filler role. These results have good agreement with the ones reported by Al-Homidy et al. (2016).

The results of the standard Proctor compaction tests with 24 h delay show that with adding cement to MS, the maximum dry unit weight decreases and the OMC increases. The reason for the decrease in the maximum dry unit weight may be related to the fact that for the materials which are compacted immediately after mixing, the change in compaction characteristics is mainly due to the change in soil gradation. However, when compaction is carried out with delay, hydration products lead to the bonding of the particles, and it is necessary to break these bonds for compaction. Hence, part of the compaction energy is used to overcome the cementation products which results in the decrease in the maximum dry unit weight. The reason for the increase in OMC is that the cement in the soil absorbs water within 24 h which leads to the increase in the OMC of the soil–cement mixture. Therefore, it is advisable to reduce the delay time

between mixing and soil compaction as much as possible in soil stabilization operations to increase soil performance and to achieve the desired compaction with less energy and moisture. Moreover, Osinubi and Nwaiwu (2006) showed that when the cemented material comes into contact with the soil, part of the hydration process begins immediately. Therefore, any delay after mixing of the sample allows the formation of stiff mass and prevents further mixing and compaction.

As it can be observed in Fig. 3, the results of the standard Proctor compaction tests for each combination in comparison with other ones have the negligible difference. Therefore, the average of the maximum dry unit weight and OMC of the MS, as well as the soil stabilized with different cement contents (for immediate condition) were used for preparation of the samples. Table 7 shows the average values of

Table 7 Average values of maximum dry unit weight and OMC for MS with different cement contents

Cement content (%)	Maximum dry unit weight (kN/m3)		OMC (%)	
	Immediate	24 h delay	Immediate	24 h delay
0	17.98		11.18	
4	18.33	17.55	10.68	13.94
6	18.50	17.31	10.33	15.29
8	18.66	17.05	10.03	17.28

the maximum dry unit weight and OMC, for MS and the cemented soil (in two conditions of immediate and with 24 h delay).

3.2 Unconfined Compressive Strength Tests

According to Fig. 4, it is observed that for a constant percentage of cement, the UCS increases with the increase in curing time. For example, for MS with 4% cement, the UCS increases by 9% and 31% with increase in curing time from 7 to 14 and from 14 to 28 days, respectively. Moreover, at the constant curing time, the UCS increases with increase in percentage of cement. Similar results were presented by Ghadakpour et al. (2020). For example, at the curing time of 7 days, it is observed that with the increase in cement percentage from 4 to 6% and from 6 to 8%, the UCS increases by 120% and 52%, respectively. There are two reasons for the mechanism of strength increase:

1. During the hydration process, the bonding between the soil particles stabilized with cement increases with the increase in curing time.
2. Cement-stabilized MS crystals strengthen the MS structure. Moreover, other researchers have reported similar results (Xing et al., 2009; Horpibulsuk et al., 2010, 2011). In other words, with adding cement to the MS, two major chemical reactions dominate the stabilization process. Firstly, the chemical reaction between cement and water, which includes calcium silicate hydrates (C–S–H), calcium aluminate hydrates (C–A–H), and calcium hydroxide (Ca(OH)$_2$). Secondly, the pozzolanic reactions between the released lime in the cement and the soil particles lead to the formation of additional C–S–H and C–A–H. These results are in agreement with the ones reported by Eskisar (2015). On the other hand, with adding cement to the MS, the behavior of the samples becomes brittle. In general, the improvement of cement-stabilized MS depends on the chemical reactions between the MS particles and the cement. Figure 4 shows that at the constant curing time, there is a linear relationship between the UCS and the percentage of cement, which has an acceptable correlation coefficient (R^2).

The influence of NC and cement on the UCS of samples at the age of 7 days is shown in Fig. 5 (in which NC as an additive = Add and NC as a replacement = Rep). According to Fig. 5, for the sample with 4% cement, the UCS decreases with the addition and replacement of different NC percentages so that the lowest the UCS was obtained for the sample with 2% NC as an additive. In other words, with adding 2% NC, the UCS decreases by 17% compared to the non-NC cemented sample. Also, for the sample with 6% cement, with the addition and replacement of NC, the UCS decreases in comparison with the non-NC cemented sample so that with replacing 2% NC, the UCS decreases by 25% compared to the non-NC cemented sample. For sample with 8% cement, with replacing 0.5% NC with cement, the highest UCS is obtained, which is 9% more than the one found for the non-NC cemented sample. It should be noted that for the mentioned percentage of cement, with replacing 2% NC, the UCS is 11% less than the non-NC cemented sample, which has the lowest the UCS.

**Fig. 4** Variation of UCS with cement content for different samples
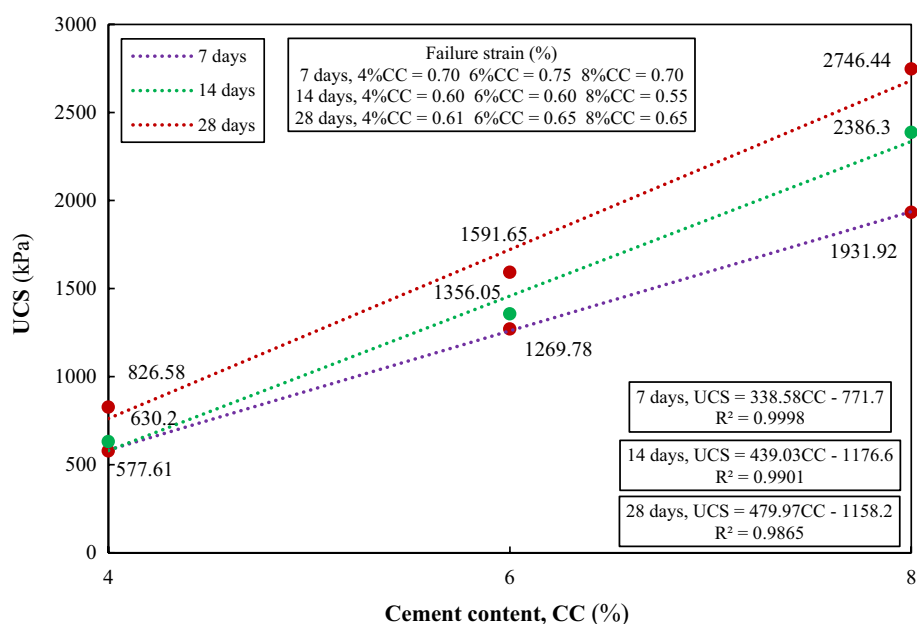
Fig. 5 Effect of NC and cement on the UCS at the 7 days curing
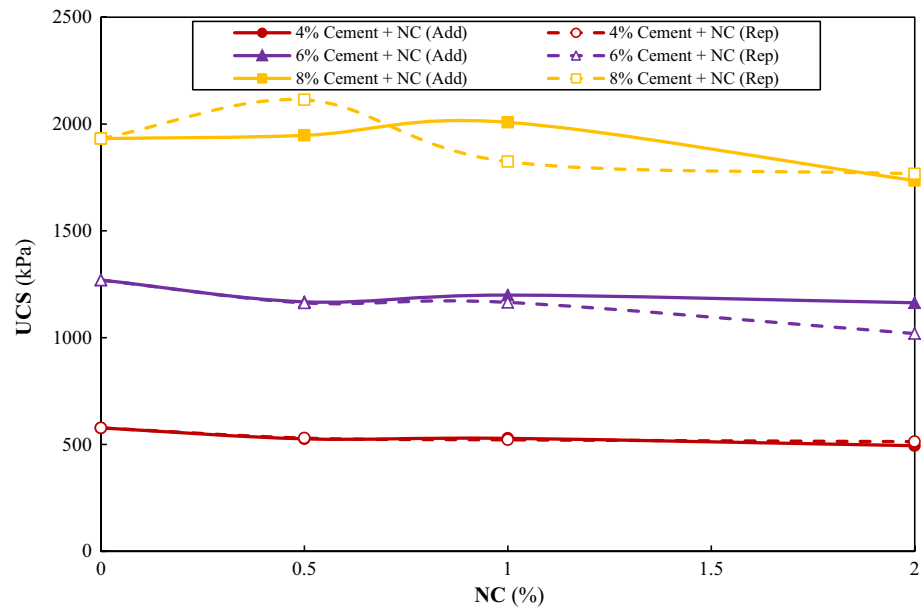
Regarding the high surface to volume ratio of crystals of NC particles, they are expected to rapidly react with $Ca(OH)_2$ and form C–S–H gel, which leads to the increase in UCS with the addition of NC. In this reaction, the size and amount of calcium crystals reduce and the resulting C–S–H increases the strength of specimens by filling the voids and increasing the density of the bond between the cement matrix and MS. These results have good agreement with the ones reported by Kafi et al. (2016). Nanoparticles with void-filling properties in C–S–H gel can contribute to the formation of a more compacted matrix. They can act as cores in the framework of the gel and produce a strong bond with the gel particles. Therefore, the stability of hydration products and the mechanical characteristics of the samples improve. Similar results were presented by Kafi et al. (2016).

Decrease in UCS by the addition of NC is related to the fact that using high amount of nanoparticles can result in the formation of weak bonds in the matrix and agglomeration of clay nanoparticles, as also observed by other researchers (Kafi et al., 2016; Hakamy et al., 2013; Kuo et al., 2006). Figure 6 shows that agglomeration occurs by adding high amount of nanoclay to the cemented soil. Thus, the excess addition of nanoparticles increases the porosity of the matrix and forms weak areas in the microstructure, which leads to the reduction of the mechanical properties. Similar results were found by previous researchers (Hosseini et al., 2010, 2014).

Figure 7 shows the total results of UCS for cemented samples with NC. As can be seen, for the constant percentage of cement and NC (as an additive and replacement), the UCS increases with increase in curing time. Also, at the constant curing time and the NC percentage, the UCS increases with increase in the percentage of cement.
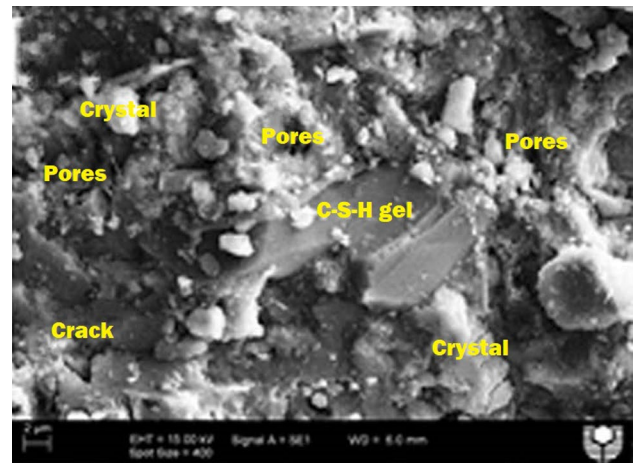
Fig. 6 Agglomeration of nanoclay (Hakamy et al. 2013)

Regarding the failure strain of cemented samples with the addition and replacement of NC, it can be stated that the cemented samples with and without NC show similar behaviors. In other words, NC does not affect the brittle behavior of cemented samples and does not change their behavior into the ductile one. Figure 8 shows the failure of the cemented samples containing the NC in the UCS test. As seen, the behavior of the samples will be more brittle with increasing curing time.

3.3 UU Triaxial Tests

The results of UU triaxial tests including stress–strain curves, as well as failure envelopes in (τ-σ) and (p-q) spaces for various samples were plotted to determine the shear strength
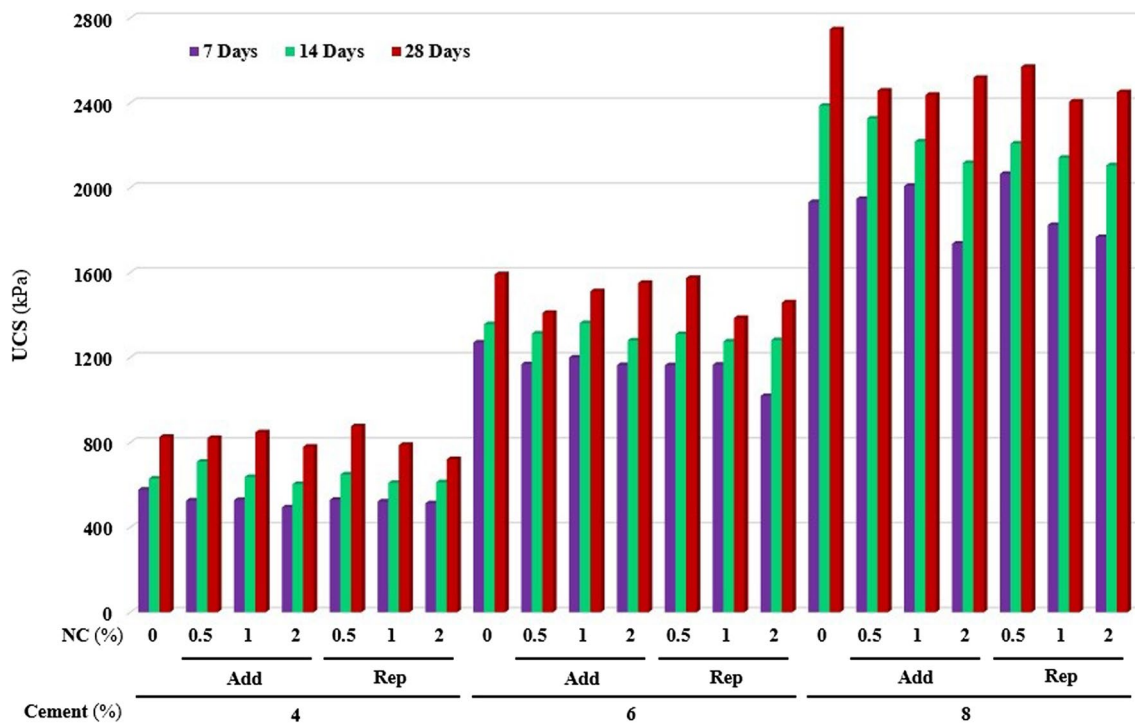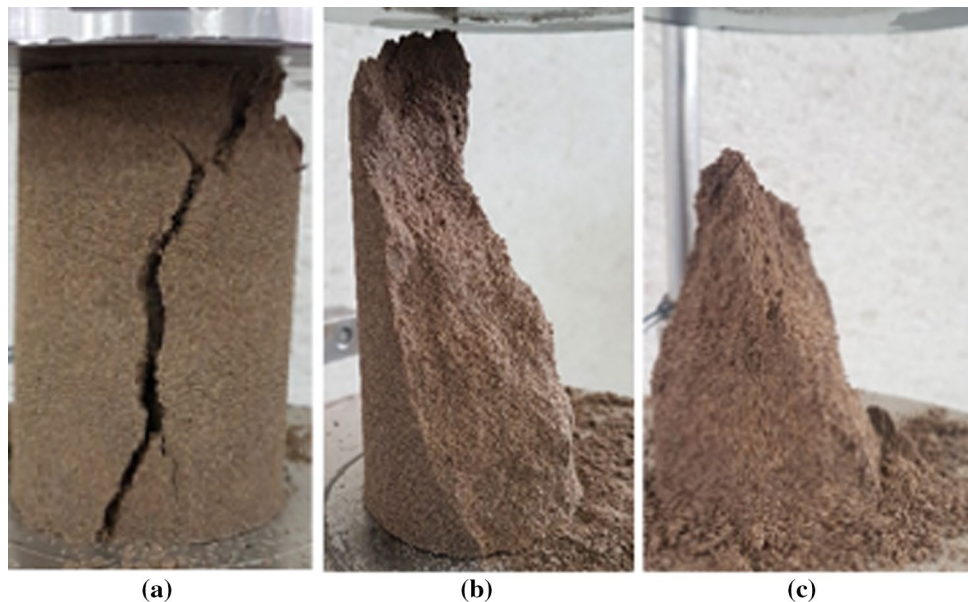
Fig. 7 Influence of the curing time, cement and NC on the UCS

**Fig. 8** Failure of the cemented samples containing the NC: a 7 days, b 14 days, and c 28 days

(a)   (b)   (c)

parameters (C and φ). It should be noted that the parameters p and q are calculated according to Eqs. (1) and (2), in which p, q, σ_1, and σ_3 are the mean stress, differential stress, major principal stress, and minor principal stress, respectively (Lambe and Whitman, 1969; Craig, 2004):

$$p = \frac{\sigma_1 + \sigma_3}{2} \tag{1}$$

$$q = \frac{\sigma_1 - \sigma_3}{2} \tag{2}$$

Figure 9 and Table 8 show one of the stress–strain curves and the total results of the tests, respectively. Figure 10 indicates triaxial parameters in (τ-σ) space for different specimens. Also, Fig. 11 shows triaxial parameters in (p–q) space. Moreover, the variation of the E_{50} and the

Fig. 9 Stress–strain curves for MS and stabilized samples with different percentages of cement under CP of 600 kPa
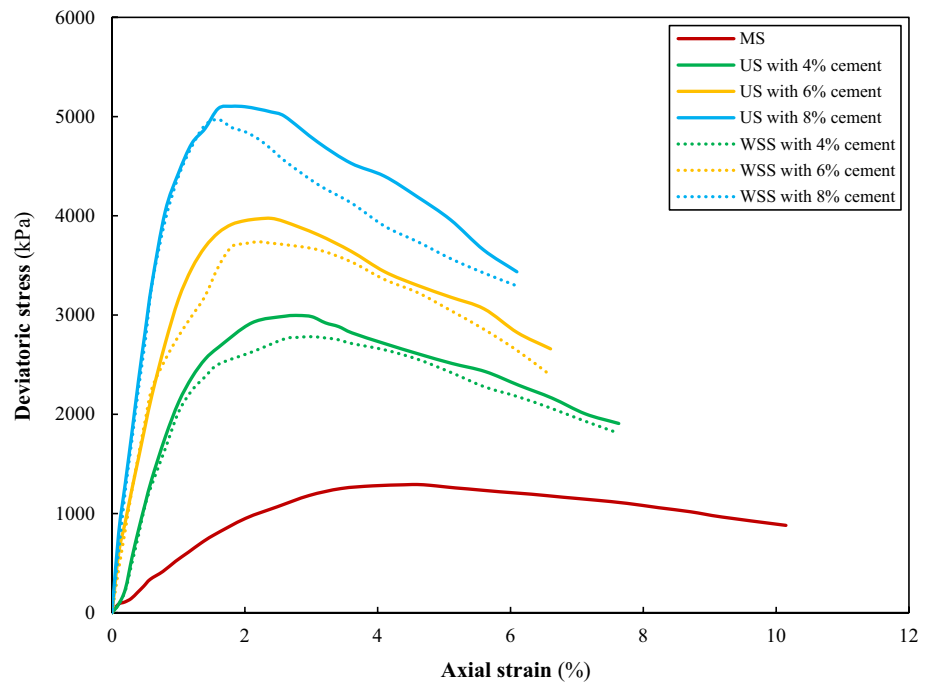
Table 8 Maximum deviatoric stress and failure strain values for various samples

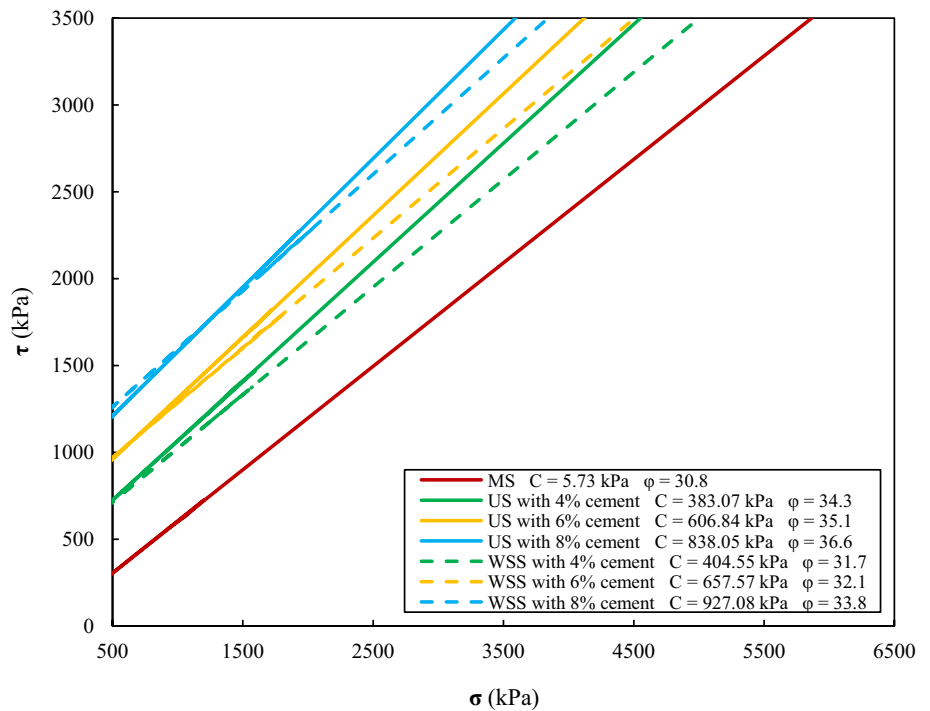| Cement content (%)	Sample type	MDS* at CP (kPa)			Equation	R2	Failure strain (%)		
		600	700	800			600	700	800
0	–	1292.19	1470.65	1711.31	MDS = 2.0956CP + 24.463	0.9927	4.97	4.78	4.60
4	US	2995.47	3288.34	3513.53	MDS = 2.5903CP + 1452.6	0.9943	2.82	2.81	3.02
	WSS	2781.94	3004.98	3226.01	MDS = 2.2204CP + 1452.2	0.9996	3.00	3.21	3.41
6	US	3973.99	4205.95	4513.79	MDS = 2.6990CP + 2341.9	0.9935	2.40	2.40	2.21
	WSS	3737.69	3998.08	4193.46	MDS = 2.2789CP + 2381.2	0.9933	2.20	2.41	2.61
8	US	5103.50	5380.06	5692.33	MDS = 2.9442CP + 3331.1	0.9988	1.80	2.00	1.80
	WSS	4969.26	5237.67	5470.27	MDS = 2.5051CP + 3472.2	0.9983	1.60	1.80	1.80

*Maximum deviatoric stress

energy absorption capacity with the percentage of cement under different CPs are shown in Fig. 12. According to Table 8, with the addition of cement to the MS, the maximum deviatoric stress increases while the failure strain decreases. In other words, although cementation increases the strength, it reduces the failure strain and makes the behavior of the samples brittle, which have also been recognized by other researchers (Choobbasti et al., 2018; Koutenaei et al., 2019). On the other hand, the US samples have a higher maximum deviatoric stress than WSS samples. The reason for the decrease in the maximum deviatoric stress with the submersion of the samples in the water is the increase in the degree of saturation. These results have good agreement with the ones found by Toll and Rahman (2017). Table 8 shows the correlations between the maximum deviatoric stress and CP values. It is observed that the maximum deviatoric stress increases linearly with
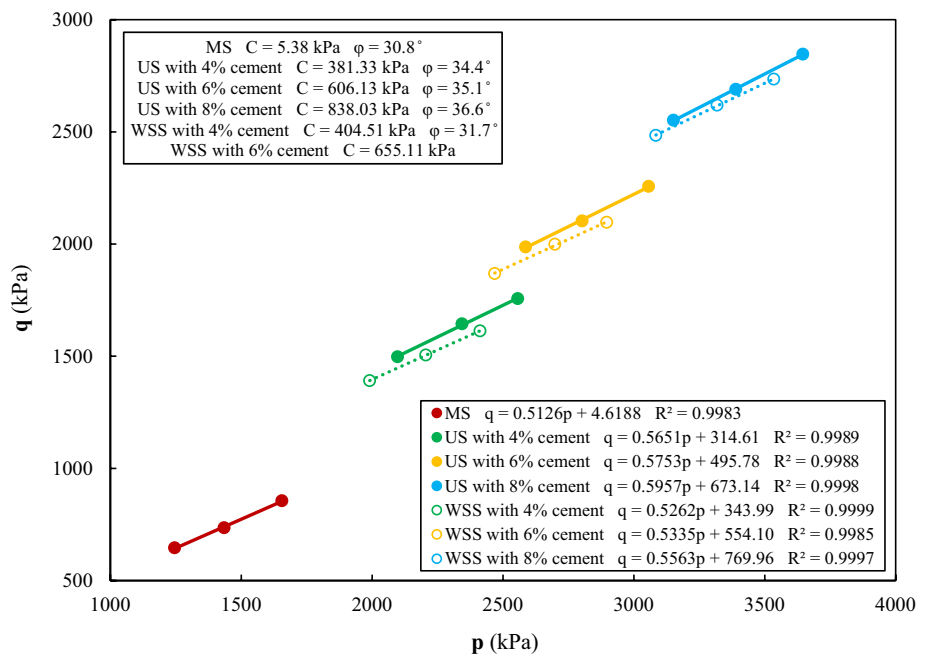
increase in CP, and there is an acceptable correlation coefficient (R^2) between them.

As presented in Figs. 10 and 11, for the MS, the C parameter has a small value while the φ has a significant value. These results have good agreement with the ones reported by Noorzad and Delavar (2019). The amount of φ obtained for the MS is in good agreement with that reported by Bowles (1995). It is also observed that in US and WSS samples, with increase in the percentage of cement, the shear strength of the samples increases which is due to the increase in the C and the φ parameters. Adding cement to MS produces a bond between the particles, resulting in the formation of grains with the larger diameters. Since interlocking of particles increases with the addition of cement to MS, a higher dilation rate is created during loading, which results in the increase of the φ. Moreover, cement has the ability to stick particles to each other through chemical reactions. Thus,

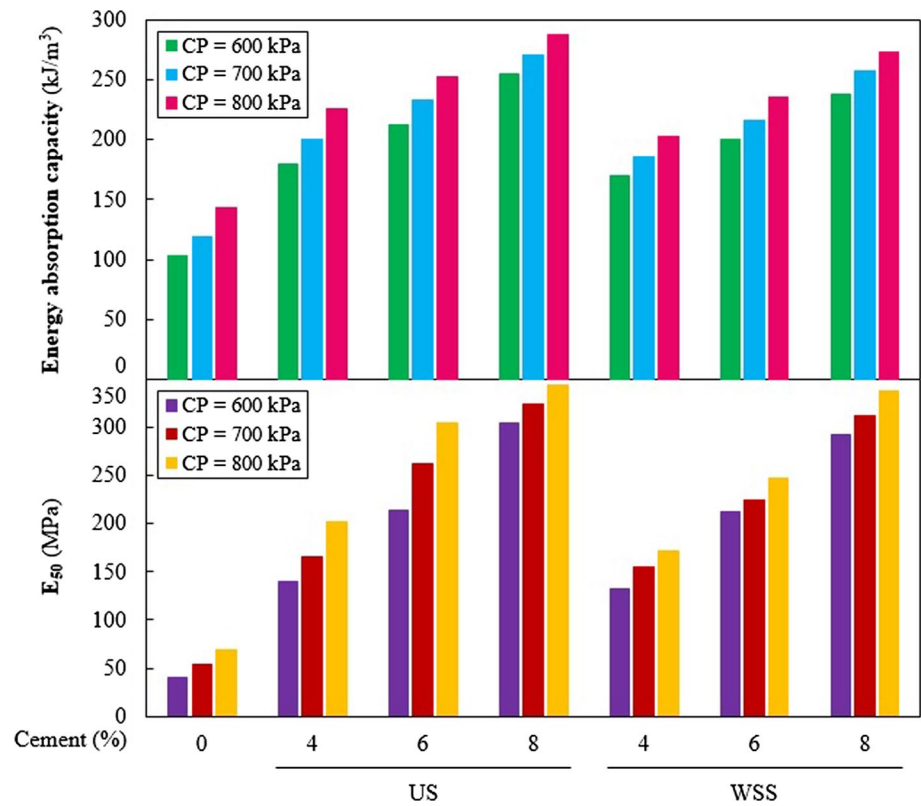**Fig. 10** Failure envelopes in (τ-σ) space for different specimens

Legend:
MS   C = 5.73 kPa φ = 30.8
US with 4% cement   C = 383.07 kPa φ = 34.3
US with 6% cement   C = 606.84 kPa φ = 35.1
US with 8% cement   C = 838.05 kPa φ = 36.6
WSS with 4% cement   C = 404.55 kPa φ = 31.7
WSS with 6% cement   C = 657.57 kPa φ = 32.1
WSS with 8% cement   C = 927.08 kPa φ = 33.8

Fig. 11 Failure envelopes in (p-q) space for various samples

MS   C = 5.38 kPa φ = 30.8°
US with 4% cement   C = 381.33 kPa φ = 34.4°
US with 6% cement   C = 606.13 kPa φ = 35.1°
US with 8% cement   C = 838.03 kPa φ = 36.6°
WSS with 4% cement   C = 404.51 kPa φ = 31.7°
WSS with 6% cement   C = 655.11 kPa

Legend:
MS $q = 0.5126p + 4.6188$ $R^2 = 0.9983$
US with 4% cement $q = 0.5651p + 314.61$ $R^2 = 0.9989$
US with 6% cement $q = 0.5753p + 495.78$ $R^2 = 0.9988$
US with 8% cement $q = 0.5957p + 673.14$ $R^2 = 0.9998$
WSS with 4% cement $q = 0.5262p + 343.99$ $R^2 = 0.9999$
WSS with 6% cement $q = 0.5335p + 554.10$ $R^2 = 0.9985$
WSS with 8% cement $q = 0.5563p + 769.96$ $R^2 = 0.9997$

the C increases with increase in cement percentage, as also observed by other researchers (Wang and Leung, 2008a; Baxter et al., 2011). In other words, [Ca(OH)$_2$] and calcium carbonate (CaCO$_3$) provide the soil–cement mixture with interesting basic properties, and C–S–H, as a major constituent of Portland cement, is responsible for the main properties of C and sustainability of soil–cement mixture. These results have good agreement with the ones reported by Mengue et al. (2017b). Moreover, it has been observed that the WSS samples have more C and less φ than US samples. The reason for the increase in the C is due to the better hydration of the cement by submerging samples in water. Also, the reason for the decrease in the φ can be due to the easier slippage of MS particles on each other in the presence of water. In addition, Toll and Rahman (2017) reported similar results. It was also observed that for cemented samples (in both usual

Fig. 12 Variation of the E50 and the energy absorption capacity with cement content for various samples under different CPs

3.3.1 E_{50} and Energy Absorption Capacity

One of the design parameters in the geotechnical engineering that indicates the amount of deformation is the E_{50}. This parameter in the triaxial test can be calculated using the slope of the line of the stress–strain curve. The corresponding point with 50% of the maximum deviatoric stress is connected to the origin of the coordinates and the corresponding strain of the desired point is found. As a result, E_{50} is determined. According to Fig. 12, it is observed that for example, with the addition of 4% cement to MS under CP of 600 kPa, the amount of E_{50} for US and WSS samples increases by 3.5

and water-submerged conditions), although the CPs were considered as high as possible, the value of the φ is not equal to zero, which its reason was mentioned previously. Besides, high CPs (1000 kPa and more) cause the loss of cementation bonds. Therefore, higher CPs cannot be applied to the samples. Also, adding cement to MS fills the voids in it. In fact, a lower void ratio is obtained. These reasons cause the samples not to be saturated by applying the CPs considered in this study. Moreover, other researchers have found similar results (Yongfeng et al., 2012; Cheng et al., 2013). Figure 11 shows that for each sample, there is a linear relationship between the values of p and q with a high R^2. It is also observed that in the range of high CP, the failure envelope of cemented soil (such as MS) is linear.

and 3.3 times, respectively. Also, with the increase in cement percentage, the E_{50} values increase in US and WSS samples. Similar results were found by previous researchers (Hamidi and Hooresfand, 2013; Ghadakpour et al., 2019). For example, under CP of 600 kPa, with the increase in cement percentage from 4 to 6% and from 6 to 8% for US sample, the E_{50} increases by 52% and 42%, respectively. Moreover, at the mentioned CP, with the increase in cement percentage from 4 to 6% and from 6 to 8% for WSS sample, the E_{50} increases by 60% and 38%, respectively. The reason for the increase of E_{50} is related to the creation of the cementation bonds between soil particles. In other words, with the increase in cement percentage, the strength and number of cementation bonds between the particles increase.

On the other hand, with increase in cement percentage, the axial strain decreases. As a result, the E_{50} increases in US and WSS samples. For a constant percentage of cement (including US and WSS samples), the E_{50} increases with increase in CP. For example, for the US sample with 4% cement, with the increase in CP from 600 to 700 kPa and from 700 to 800 kPa, the E_{50} increases by 18.5% and 21.5%, respectively. Moreover, for the WSS sample at the mentioned percentage of cement, with the increase in CP from 600 to 700 kPa and from 700 to 800 kPa, the E_{50} increases by 17% and 11%, respectively. For a constant percentage of cement and CP, the E_{50} for US samples are higher than for WSS samples. This can be related to the fact that the

maximum deviatoric stress values of US samples are higher than the corresponding values found for WSS samples. However, there is a little difference between the corresponding strains with 50% of the maximum deviatoric stress in the US and WSS samples. Thus, the E_{50} for US samples becomes higher than WSS samples.

The energy absorption capacity expresses the energy needed to make deformation in materials. This parameter in the triaxial test is obtained by calculating the area below the stress–strain curve. According to Fig. 12, it can be seen that, for example, with the addition of 4% cement to MS under CP of 600 kPa, the amount of the energy absorption capacity for US and WSS samples increases by 75% and 65%, respectively. Also, with the increase in cement percentage, the energy absorption capacity values increase in US and WSS samples, which have also been recognized by other researchers (Choobbasti et al., 2018; Amini and Hamidi, 2014). For example, under CP of 600 kPa, with the increase in cement percentage from 4 to 6% and from 6 to 8% for US sample, the energy absorption capacity increases by 18% and 20%, respectively. Moreover, at the mentioned CP, with the increase in cement percentage from 4 to 6% and from 6 to 8% for the WSS sample, the energy absorption capacity increases by 18% and 19%, respectively.

By comparing the amounts of the energy absorption capacity for a constant percentage of cement and CP, it is observed that the amount of the energy absorption capacity in US samples is higher than WSS samples. For example, for MS with 4% cement under CP of 600 kPa, the energy absorption capacity of US is 6% higher than energy absorption capacity of WSS samples. The reason is that, for a constant percentage of cement, the axial strain at the end of the test is the same in both usual and submersion conditions (such as Fig. 9) and the deviatoric stress values of US specimens are higher than WSS specimens. As a result, the energy absorption capacity for a constant percentage of cement in US samples is more than WSS samples. It is also observed that in all specimens (including MS, US, and WSS specimens), the amount of the energy absorption capacity increases with increase in CP. Choobbasti et al. (2018) and Amini and Hamidi (2014) reported similar results. For example, for MS, with the increase in CP from 600 to 700 kPa and from 700 to 800 kPa, the energy absorption capacity increases by 16% and 20%, respectively. Moreover, for US sample with 4% cement, with the increase in CP from 600 to 700 kPa and from 700 to 800 kPa, the energy absorption capacity increases by 12% and 13%, respectively. Besides, for the WSS sample at the mentioned percentage of cement, with the increase in CP from 600 to 700 kPa and from 700 to 800 kPa, the energy absorption capacity increases by 9.5% and 9%, respectively. The increase in the energy absorption capacity with increase in CP is related to the fact that the propagation of fracture crack and deformation of the sample are limited under CP. As a result, more energy should be absorbed if the sample wants to reach its failure state. Similar results were presented by Liu and He (2012).

3.3.2 Failure of Samples

According to the failure states created in the MS and stabilized samples (Fig. 13), it is observed that in both cases, a shear band is formed. In the case of MS specimens, the reason for the formation of a shear band is related to the soil compaction. In addition, cemented samples show brittle

Fig. 13 Samples at the end of the UU triaxial tests: **a** MS sample, **b** US sample, and **c** WSS sample

(a)   (b)   (c)
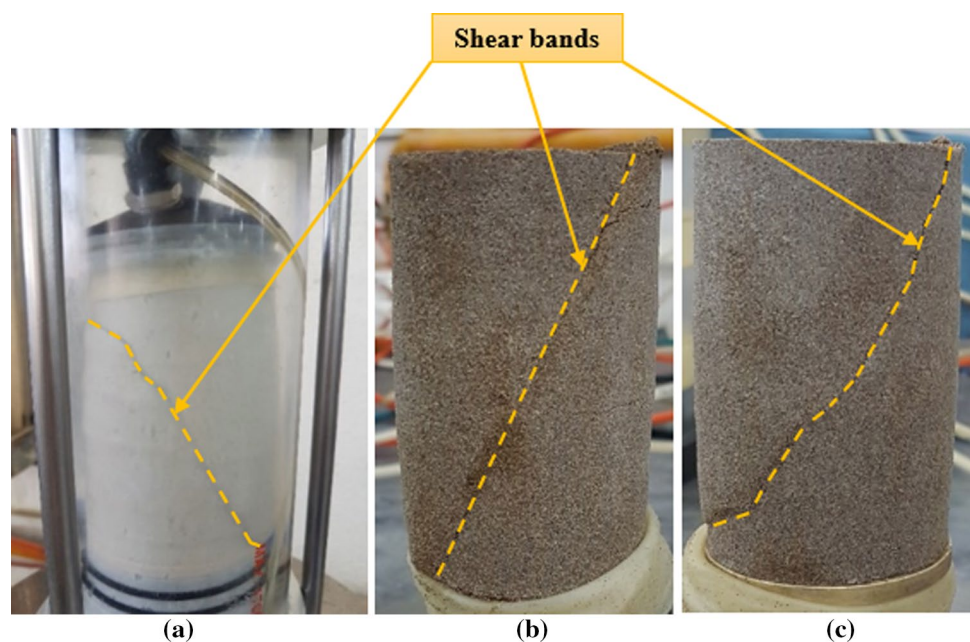
behavior, which leads to the formation of shear bands. These results have good agreement with the ones reported by Consoli et al. (2009). The formation of a shear band in the samples occurs when strain softening is observed. These results are in agreement with the ones found by Wang and Leung (2008b). In other words, the behavior of cement-stabilized specimens is similar to that of dense sands or over-consolidated clays, in which their type of failure is the formation of the shear band.

4 Conclusions

The results of this study are summarized as follows:

1. With replacing 15% silt with sand, the maximum dry unit weight increased and the OMC decreased. The denser packing, which occurs through filling the void spaces with the addition of fines, leads to the increase in the maximum dry unit weight and the reduction of OMC (less water is required to fill the voids between the sand particles).
2. With adding cement to MS, the maximum dry unit weight increased and the OMC decreased. The maximum dry unit weight increase can be due to the higher specific gravity and smaller particles of cement compared to the MS. The decrease in the OMC may be due to the self-desiccation of the water. Also, the reduction in OMC indicates that the cement acts as a lubricant as well as its filler role. On the other hand, with adding cement to MS (with 24 h delay), the maximum dry unit weight decreased and the OMC increased. In general, it is advisable to reduce the delay time between mixing and soil compaction as much as possible in soil stabilization operations to improve soil performance and to achieve the desired compaction with less energy and moisture content.
3. With the increase in cement percentage and curing time, the UCS increased. The increase in the UCS of cement-stabilized MS is due to chemical and pozzolanic reactions between soil particles and cement. Also, the cement particles are placed between soil particles, reducing empty spaces, thus increasing the contact area between the particles of soil. On the other hand, with the addition and replacement of NC to cement-stabilized MS, the UCS did not change significantly in most of the samples.
4. Adding cement makes the behavior of samples brittle, where this behavior is similar for samples with different percentages of cement. Moreover, there was no change in the brittle behavior of the cemented samples with the addition and replacement of NC.

5. With adding cement to MS, the shear strength of the samples increased, which is due to the increase in the C and φ parameters. The addition of cement to MS produced a bond between the particles, resulting in the formation of grains with the larger diameters. Since the interlocking of particles increases with the addition of cement to MS, a higher dilation rate is created during loading, which results in the increase of the φ. Moreover, cement has the ability to stick particles to each other through chemical reactions. Thus, the C increases with increase in cement percentage. Also, WSS samples have more C and less φ than US samples. The reason for the increase in C is due to the better hydration of the cement by submerging samples in water. The reason for the decrease in φ can be due to the easier slippage of MS particles on each other in the presence of water.
6. With the increase in the cement percentage and CP, in both usual and water-submerged conditions, the amounts of the E_{50} and the energy absorption capacity increased. Moreover, the values of the E_{50} and the energy absorption capacity for US samples are more than the WSS ones.

Declarations

Conflict of interest The authors confirm that there are no known conflicts of interest associated with this publication.

References

Al-Aghbari MY, Mohamedzein YEA, Taha R (2009) Stabilization of desert sands using cement and cement dust. Proc Inst Civ Eng Ground Improv 162(3):145–151. https://doi.org/10.1680/grim.2009.162.3.145

Al-Homidy AA, Dahim MH, Abd El Aal AK (2017) Improvement of geotechnical properties of sabkha soil utilizing cement kiln dust. J Rock Mech Geotech Eng 9(4):749–760. https://doi.org/10.1016/j.jrmge.2016.11.012

Amini Y, Hamidi A (2014) Triaxial shear behavior of a cement-treated sand-gravel mixture. J Rock Mech Geotech Eng 6(5):455–465. https://doi.org/10.1016/j.jrmge.2014.07.006

ASTM (2007) Standard test method for particle-size analysis of soils (withdrawn 2016). ASTM International. D422-63(2007)e2, West Conshohocken, PA. doi: https://doi.org/10.1520/D0422-63R07E02

ASTM (2012) Standard test methods for laboratory compaction characteristics of soil using standard effort (12,400 ft-lbf/ft^3 (600 kN-m/m^3)). ASTM International. D698-12e2, West Conshohocken, PA. doi: https://doi.org/10.1520/D0698-12E02

ASTM (2014) Standard test methods for specific gravity of soil solids by water pycnometer. ASTM International. D854-14, West Conshohocken, PA. doi: https://doi.org/10.1520/D0854-14

ASTM (2015) Standard test method for unconsolidated-undrained triaxial compression test on cohesive soils. ASTM International. D2850-15, West Conshohocken, PA. doi: https://doi.org/10.1520/D2850-15

ASTM (2016) Standard test method for unconfined compressive strength of cohesive soil. ASTM International. D2166/D2166M-16, West Conshohocken, PA. doi: https://doi.org/10.1520/D2166_D2166M-16

ASTM (2017a) Standard practice for classification of soils for engineering purposes (unified soil classification system). ASTM International. D2487-17e1, West Conshohocken, PA. doi: https://doi.org/10.1520/D2487-17E01

ASTM (2017b) Standard test methods for liquid limit, plastic limit, and plasticity index of soils. ASTM International. D4318-17e1, West Conshohocken, PA. doi: https://doi.org/10.1520/D4318-17E01

ASTM (2019) Standard test methods for moisture-density (unit weight) relations of soil-cement mixtures. ASTM International. D558/D558M-19, West Conshohocken, PA. doi: https://doi.org/10.1520/D0558_D0558M-19

Baxter CDP, Sharma MSR, Moran K, Vaziri H, Narayanasamy R (2011) Use of $\bar{A} = 0$ as a failure criterion for weakly cemented soils. J Geotech Geoenviron Eng 137(2):161–170. https://doi.org/10.1061/(ASCE)GT.1943-5606.0000414

Baziar MH, Saeidaskari J, Alibolandi M (2018) Effects of nanoclay on the treatment of core material in earth dams. J Mater Civ Eng 30(10):04018250. https://doi.org/10.1061/(ASCE)MT.1943-5533.0002415

Bowles JE (1995) Foundation analysis and design, 5th edn. McGraw-Hill, New York

Cheng L, Ruwisch RC, Shahin MA (2013) Cementation of sand soil by microbially induced calcite precipitation at various degrees of saturation. Can Geotech J 50(1):81–90. https://doi.org/10.1139/cgj-2012-0023

Choobbasti AJ, Vafaei A, Kutanaei SS (2018) Static and cyclic triaxial behavior of cemented sand with nanosilica. J Mater Civ Eng 30(10):04018269. https://doi.org/10.1061/(ASCE)MT.1943-5533.0002464

Consoli NC, Vendruscolo MA, Fonini A, Rosa FD (2009) Fiber reinforcement effects on sand considering a wide cementation range. Geotext Geomembr 27(3):196–203. https://doi.org/10.1016/j.geotexmem.2008.11.005

Craig RF (2004) Craig's soil mechanics, 7th edn. Spon Press, Taylor & Francis Group, London

Deb K, Sawant V, Kiran A (2010) Effects of fines on compaction characteristics of poorly graded sands. Int J Geotech Eng 4(2):299–304. https://doi.org/10.3328/IJGE.2010.04.02.299-304

Eskisar T (2015) Influence of cement treatment on unconfined compressive strength and compressibility of lean clay with medium plasticity. Arab J Sci Eng 40:763–772. https://doi.org/10.1007/s13369-015-1579-z

Ghadakpour M, Choobbasti AJ, Kutanaei SS (2019) Investigation of the deformability properties of fiber reinforced cemented sand. J Adhes Sci Technol 33(17):1–26. https://doi.org/10.1080/01694243.2019.1619224

Ghadakpour M, Choobbasti AJ, Kutanaei SS (2020) Investigation of the Kenaf fiber hybrid length on the properties of the cement-treated sandy soil. Transp Geotech 22:100301. https://doi.org/10.1016/j.trgeo.2019.100301

Hakamy A, Shaikh FUA, Low IM (2013) Microstructures and mechanical properties of hemp fabric reinforced organoclay-cement nanocomposites. Constr Build Mater 49:298–307. https://doi.org/10.1016/j.conbuildmat.2013.08.028

Hamidi A, Hooresfand M (2013) Effect of fiber reinforcement on triaxial shear behavior of cement treated sand. Geotext Geomembr 36:1–9. https://doi.org/10.1016/j.geotexmem.2012.10.005

Hasanzadeh A, Shooshpasha I (2019) Effects of silica fume on cemented sand using ultrasonic pulse velocity. J Adhes Sci Technol 33(11):1184–1200. https://doi.org/10.1080/01694243.2019.1582890

Hasanzadeh A, Shooshpasha I (2020) Influence of silica fume on the geotechnical characteristics of cemented sand. Geotech Geol Eng. https://doi.org/10.1007/s10706-020-01436-w

Horpibulsuk S, Rachan R, Chinkulkijniwat A, Raksachon Y, Suddeepong A (2010) Analysis of strength development in cement-stabilized silty clay from microstructural considerations. Constr Build Mater 24(10):2011–2021. https://doi.org/10.1016/j.conbuildmat.2010.03.011

Horpibulsuk S, Rachan R, Suddeepong A (2011) Assessment of strength development in blended cement admixed bangkok clay. Constr Build Mater 25(4):1521–1531. https://doi.org/10.1016/j.conbuildmat.2010.08.006

Hosseini P, Booshehrian A, Farshchi S (2010) Influence of nano-SiO_2 addition on microstructure and mechanical properties of cement mortars for ferrocement. Transp Res Rec J Transp Res Board 2141(1):15–20. https://doi.org/10.3141/2141-04

Hosseini P, Hosseinpourpia R, Pajum A, Khodavirdi MM, Izadi H, Vaezi A (2014) Effect of nano-particles and aminosilane interaction on the performances of cement-based composites: an experimental study. Constr Build Mater 66:113–124. https://doi.org/10.1016/j.conbuildmat.2014.05.047

Iranpour B, Haddad A (2016) The influence of nanomaterials on collapsible soil treatment. Eng Geol 205:40–53. https://doi.org/10.1016/j.enggeo.2016.02.015

Kafi MA, Nik AS, Bahari A, Nik AS, Mirshafiei E (2016) Microstructural characterization and mechanical properties of cementitious mortar containing montmorillonite nanoparticles. J Mater Civ Eng 28(12):04016155. https://doi.org/10.1061/(ASCE)MT.1943-5533.0001671

Koutenaei RY, Choobbasti AJ, Kutanaei SS (2019) Triaxial behavior of a cemented sand reinforced with kenaf fibers. Europ J Environ Civ Eng. https://doi.org/10.1080/19648189.2019.1574607

Kuo WY, Huang JS, Lin CH (2006) Effects of organo-modified montmorillonite on strengths and permeability of cement mortars. Cem Concr Res 36(5):886–895. https://doi.org/10.1016/j.cemconres.2005.11.013

Kutanaei SS, Choobbasti AJ (2017) Effects of nanosilica particles and randomly distributed fibers on the ultrasonic pulse velocity and mechanical properties of cemented sand. J Mater Civ Eng 29(3):04016230. https://doi.org/10.1061/(ASCE)MT.1943-5533.0001761

Lambe TW, Whitman RV (1969) Soil mechanics, 1st edn. London, Wiley

Liu E, He S (2012) Effects of cyclic dynamic loading on the mechanical properties of intact rock samples under confining pressure conditions. Eng Geol 125:81–91. https://doi.org/10.1016/j.enggeo.2011.11.007

Mengue E, Mroueh H, Lancelot L, Eko RM (2017a) Physicochemical and consolidation properties of compacted lateritic soil treated with cement. Soils Found 57(1):60–79. https://doi.org/10.1016/j.sandf.2017.01.005

Mengue E, Mroueh H, Lancelot L, Eko RM (2017b) Mechanical improvement of a fine-grained lateritic soil treated with cement for use in road construction. J Mater Civ Eng 29(11):04017206. https://doi.org/10.1061/(ASCE)MT.1943-5533.0002059

Moon SW, Vinoth G, Subramanian S, Kim J, Ku T (2020) Effect of fine particles on strength and stiffness of cement treated sand. Granul Matter 22(9):1–13

Noorzad R, Delavar IN (2019) Investigation into the short-term behavior of silty sand stabilized with colloidal silica. Sci Iran A 26(3):1206–1213

Osinubi KJ, Nwaiwu CMO (2006) Compaction delay effects on properties of lime-treated soil. J Mater Civ Eng 18(2):250–258. https://doi.org/10.1061/(ASCE)0899-1561(2006)18:2(250)

Sariosseiri F, Muhunthan B (2009) Effect of cement treatment on geotechnical properties of some Washington State soils. Eng Geol 104(1–2):119–125. https://doi.org/10.1016/j.enggeo.2008.09.003

Schnaid F, Prietto PDM, Consoli NC (2001) Characterization of cemented sand in triaxial compression. J Geotech Geoenviron Eng 127(10):857–868. https://doi.org/10.1061/(ASCE)1090-0241(2001)127:10(857)

Shahidi M, Farrokhi F, Asemi F (2019) Changes in physical and mechanical properties of gas oil-contaminated clayey sand after addition of clay nanoparticles. J Environ Eng 145(4):04019004. https://doi.org/10.1061/(ASCE)EE.1943-7870.0001508

Tabarsa A, Latifi N, Meehan CL, Manahiloh KN (2018) Laboratory investigation and field evaluation of loess improvement using nanoclay – a sustainable material for construction. Constr Build Mater 158:454–463. https://doi.org/10.1016/j.conbuildmat.2017.09.096

Toll DG, Rahman ZA (2017) Critical state shear strength of an unsaturated artificially cemented sand. Géotechnique 67(3):208–215. https://doi.org/10.1680/jgeot.15.P.042

Vranna A, Tika T (2020) Undrained monotonic and cyclic response of weakly cemented sand. J Geotech Geoenviron Eng 146(5):04020018. https://doi.org/10.1061/(ASCE)GT.1943-5606.0002246

Wang YH, Leung SC (2008a) Characterization of cemented sand by experimental and numerical investigations. J Geotech Geoenviron Eng 134(7):992–1004. https://doi.org/10.1061/(ASCE)1090-0241(2008)134:7(992)

Wang YH, Leung SC (2008b) A particulate-scale investigation of cemented sand behavior. Can Geotech J 45(1):29–44. https://doi.org/10.1139/T07-070

Xing H, Yang X, Xu C, Ye G (2009) Strength characteristics and mechanisms of salt-rich soil-cement. Eng Geol 103(1–2):33–38. https://doi.org/10.1016/j.enggeo.2008.07.011

Yongfeng D, Songyu L, Jian'an H, Kan L, Yanjun D, Fei J (2012) Strength and permeability of cemented soil with PAM. In: proceedings of the 4th international conference on grouting and deep mixing, 15–18 February, New Orleans, Louisiana, United States, pp 1800–1807

Zhang G (2007) Soil nanoparticles and their influence on engineering properties of soils. Geo-Denver 2007, 18–21 February, Denver, Colorado, United States, pp 1–13. Doi: https://doi.org/10.1061/40917(236)37

Zomorodian SMA, Shabnam M, Armina S, O'Kelly BC (2017) Strength enhancement of clean and kerosene-contaminated sandy lean clay using nanoclay and nanosilica as additives. Appl Clay Sci 140:140–147. https://doi.org/10.1016/j.clay.2017.02.004